



The solar noise barrier project: 1. Effect of incident light orientation on the performance of a large-scale luminescent solar concentrator noise barrier



Michalis Kanellis^a, Minne M. de Jong^b, Lenneke Slooff^c, Michael G. Debije^{d,*}

^a Smart Energy Buildings & Cities, Eindhoven University of Technology, 5600 MB Eindhoven, The Netherlands

^b Solar Energy Application Centre, 5656 AE Eindhoven, The Netherlands

^c Energy Research Centre of the Netherlands (ECN), 1755 ZG Petten, The Netherlands

^d Dept. Chemical Engineering & Chemistry, Eindhoven University of Technology, 5600 MB Eindhoven, The Netherlands

ARTICLE INFO

Article history:

Received 19 May 2016

Received in revised form

7 October 2016

Accepted 31 October 2016

Available online 1 November 2016

Keywords:

Luminescent solar concentrator

Demonstrator

Noise barrier

Solar energy

ABSTRACT

In this work we describe the relative performance of the largest luminescent solar concentrator (LSC) constructed to date. Comparisons are made for performance of North/South and East/West facing panels during a sunny day. It is shown that the East/West panels display much more varied performance during the day, as the structural elements of the barrier interfere with solar illumination and cause shading, but perform similarly for both front and back illumination conditions. The results of a more extended, 200 day measurement period mirror the results of the single sunny day results. This work demonstrates the importance of frame design to minimize self-shading of the LSC panels.

© 2016 The Authors. Published by Elsevier Ltd. This is an open access article under the CC BY license (<http://creativecommons.org/licenses/by/4.0/>).

1. Introduction

Exploiting the potential of solar energy in a city setting has proven to be a challenge. There are a number of research efforts currently dedicated to developing next generation urban solar panels. Research on shade tolerant panels, increasing the freedom of shape of the PV and introduction of color are all steps towards bringing solar PV into a built environment on the large scale [1,2].

An alternative solar energy generator which could find extensive use in the urban setting is the luminescent solar concentrator, or LSC. The LSC has had a long history in the scientific and patent literature since first being described in the late 1970's [3–6]. The LSC is a relatively simple concept for a solar energy generator: it usually is manifested as a polymer plate filled with fluorescent molecules that absorb incident sunlight. The fluorophores re-emit the light at a longer wavelength, a fraction of which is trapped by total internal reflection in the polymer plate by virtue of its high refractive index. The trapped light is thus directed towards the narrow edges of the plate, where long, thin photovoltaic (PV) cells

are placed to convert the emission light into electricity. The LSC has several potential advantages which make it interesting for integration in the built environment. The aesthetics of the device can hold appeal for their color [7] and potential to be of almost any shape. The LSC is able to function as either opaque or translucent objects. They function similarly in direct and indirect sunlight [8], and are relatively robust. While current electrical generation efficiencies are modest [9,10], their reduced cost and potential for huge area coverage as well as their ability to be used as construction elements reduce the importance of the absolute efficiency.

Despite decades of research and considerable advances in materials and design concepts, there have been few examples of any efforts to scale up an LSC device for outdoor application for longer-term monitoring. Both a liquid-based and a solid polymer LSC were installed outdoors in Egypt and their performances were followed for the period of two weeks [11] and over summers [12,13]. Smaller sheets were studied in Northern Europe climates for close to 300 days [5], and a $20 \times 8 \text{ cm}^2$ dye topped polymer plate in Riyadh, Saudi Arabia for one year [14]. A number of other semi-commercial efforts have been attempted, but the results were never made public.

With this in mind, we developed the Solar Noise Barrier (SONOB) program to tackle the issues related to production of a

* Corresponding author.

E-mail address: m.g.debije@tue.nl (M.G. Debije).

larger-scale LSC device, and to monitor its performance under the harsh conditions of a Dutch year. SONOB resulted in the construction of 2 noise barrier modules, each $4 \times 5 \text{ m}^2$ and 12 mm thick, one facing East/West and the other North/South. The modules each consisted of 4 separate $1 \times 5 \text{ m}^2$ panels. Two were clear glass plates 8 mm thick embedded with silicon PV cells, and two dye-embedded LSC devices, one containing an apparent orange and one an apparent red colored fluorescent dye. Since the early spring of 2015 we have been monitoring a number of parameters related to the barrier electrical performance, including the output of the 16 PV cell strings located about the top and bottom sides of each of the LSCs, the PV cells of the PV embedded glass plates, wind speeds, cell temperatures and illumination conditions at 2 min intervals.

During the day the sun is in continual motion across the sky, and presents the LSC panels a variety of illumination conditions. There are a host of other factors potentially contributing to the performance of the panels including the effects of clouds, soiling, shadowing, graffiti, and temperature. By understanding how the panels respond to the various light incidence conditions, future designs can focus on the aspects that underperformed of the installed panels in order to solve these deficiencies and improve overall performance of the device. In this paper, we discuss the effect of solar position on the outputs of the LSC sheets on a particularly sunny day and compare to some longer-term measurements.

2. Materials and methods

Four cast PMMA plates $1 \times 5 \times 0.012 \text{ m}^3$ were used in the experimental setup. Two plates contained the fluorescent dye Lumogen Red305 and two plates contained the fluorescent dye Lumogen Orange240 (both dyes from BASF) [15]. The top and bottom edges of the panels were attached with two strips of series connected cells, each containing seven $12 \times 78 \text{ mm}^2$ monocrystalline silicon PV cells (SolTech). These strip pairs were mounted at four different locations on the LSC plate, labelled TS (Top, Side), TM (Top, Middle), BM (Bottom, Middle) and BS (Bottom, Side) by an optically transparent silicone-based flexible glue. White tape was used to mask the overhang to the edge of the LSC lightguide plate. Each of the four cell strip pairs was monitored independently for performance. The two vertical edges on each LSC panel were affixed with a white scatterer. The temperature of some of the cells was monitored during the experiments by attached thermocouples (T-type from Omega Engineering).

Two noise barrier assemblies were created, each consisting of four panels: one each of the red and orange dye, and two glass panels containing silicon PVs from Scheuten solar. The red panel was on top, the orange below this, and the two bottom panels being the silicon based PV panels, as may be seen in Fig. 1. The assembly of the panels, cells, and requisite wiring and encasement in an aluminum frame were overseen by Van Campen Industries. The two assembled noise barriers were installed by Heijmans with one



Fig. 1. Photographs of the noise barrier prototypes. (Left) Both panels are visible. (Right) The East/West facing barrier.

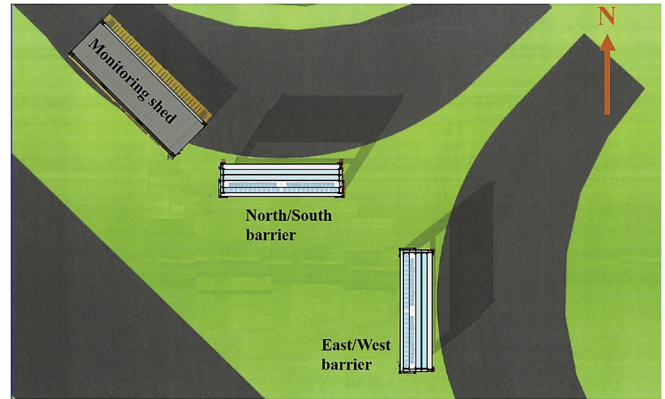


Fig. 2. Location map for the installation site in s' Hertogenbosch, the Netherlands.

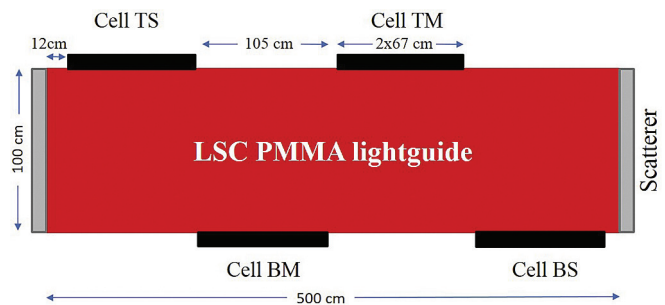


Fig. 3. Schematic of the LSC device, including attachment points of the photovoltaic cells labelled TS (Top, Side), TM (Top, Middle), BM (Bottom, Middle) and BS (Bottom, Side).

barrier facing North/South and the other East/West along a major traffic conduit in the city of Den Bosch, the Netherlands (see Fig. 2). The tilts were such that the barriers reclined 15° towards the north and east, respectively. The barriers' wiring was completed and attached to the various detectors used in the experiments and the controlling computer by SEAC. Two EKO MS-802 pyrometers were mounted atop both the barriers, in plane with the front and rear side of the barrier to collect information on irradiance. The output of the PV cells was monitored by an EKO MP-160 IV tracer in combination with a number of switching units.

3. Results and discussion

In this work we will focus discussion on only the performance of the Red305 doped polymeric sheets [9,10,15]. The top middle (TM) and bottom middle (BM) cells, top side (TS) and bottom side (BS) cells (see Fig. 3) will be compared in this work for both the North/South and East/West facing panels.

The cells' performance ratios were compared on a very sunny day (June 30, 2015) when no cloud was registered in the sky above Den Bosch, The Netherlands. An image depicting the solar path during this day is depicted as Fig. 4 below.

The definition of the performance ratio, PR , which we use to compare the output of all the cells attached to the LSC is:

$$PR = \frac{\text{Field Efficiency}}{\text{Theoretical Efficiency}} = \frac{P_{\text{measured}}(W)}{P_{\text{rated}}(W)} \times \frac{E_{\text{stc}}(W/m^2)}{E_{\text{measured}}(W/m^2)} \quad (1)$$

where $E_{\text{stc}} = 1000 \text{ W/m}^2$, P_{measured} was determined from the

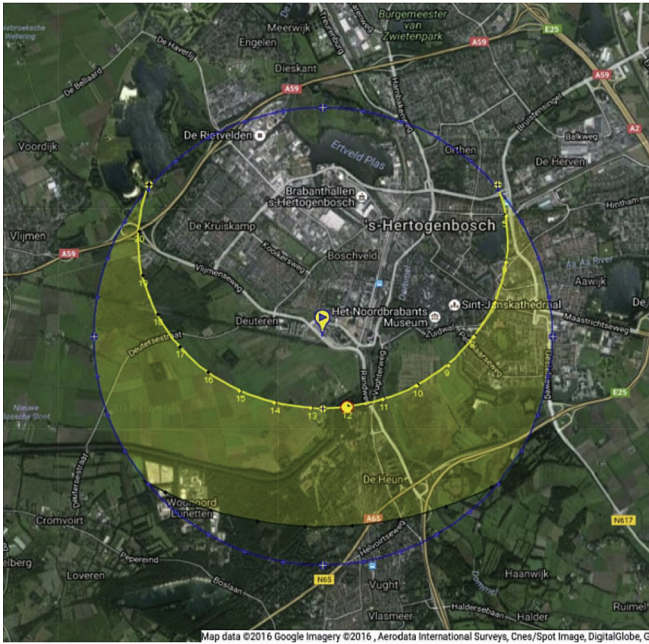


Fig. 4. Depiction of the solar path over the noise barrier installation location for June 30, 2015. Data copied from SunEarthTools.com.

maximum power point on its IV curve, and P_{rated} was the nominal power outputs of the cell, and $E_{measured}$ is the total measured irradiance from both sides of the LSC panel at the test site. The fill factors were around 80% for the PVs. While not a perfect parameter to describe LSC performance (for example, cell heating can influence the measured power), the PR should give a reasonable comparison between cell performances given similar weather and lighting conditions. It should be noted the results given in this paper are based on single panels. Less emphasis should be placed on comparing absolute numbers of PV cell strips but more on the relative performance of individual cell strips throughout a measurement period: there are variations between the strips arising from differences in the optical connection between the polymer plate and the cell strips.

3.1. Middle: top vs bottom cells

The silicon photovoltaic cells that are compared here correspond to TM and BM cells in Fig. 2 for both the East/West and North/South facing noise barriers. The performance ratio comparison for these two cases is shown in Fig. 5.

For the East/West facing noise barriers, it is clear that the BM part of the LSC panel receives more light during the first half of the

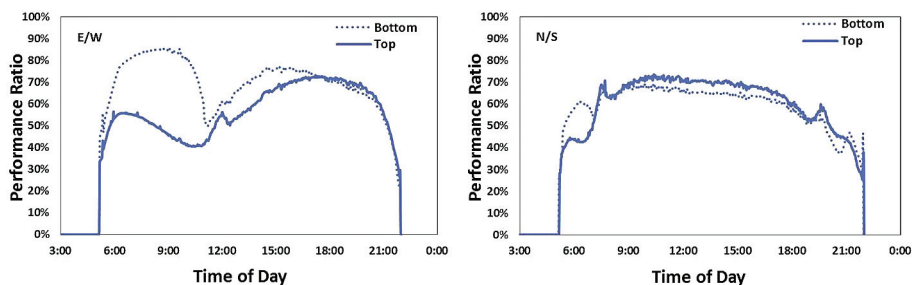


Fig. 5. Performance ratios of silicon PV cells mounted on the BM (dotted lines) and TM (solid lines) for barriers facing east/west (E/W) and north/south (N/S) as a function of the time of day on June 30, 2015.

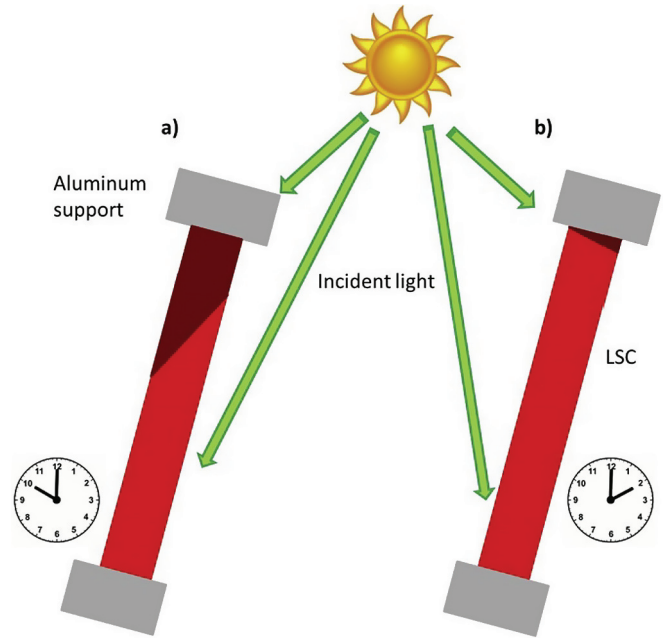


Fig. 6. Effect of solar position on shading of the East/West facing LSC noise barrier panels. a) At 10:00, the top aluminum support (with its relative size exaggerated in the image) shades the top panel area closest to the attached PV cells but has little effect on the bottom of the panel or attached cell. b) At 14:00 the sun is now facing the front of the panel, and there is much less shading of either the top or bottom.

day (until solar noon): during this time the sunlight approaches from the rear side of the panel. The dramatic difference in the performance during the early hours in Fig. 5a is ascribed to the effect of frame shading as the sun passes over the metal top bar. The transport distance of dye-emitted light in the LSC can be quite limited by reabsorption events resulting from the limited Stokes shift of the dyes (there is general spectral overlap between the absorption and emission spectra of the dyes), internal scattering, and even parasitic absorption by the polymeric lightguide [16].

The sunlight approaches the East/West facing barrier from the rear side in the morning: the panel tilts 15° towards the East. The incident light approaching the top of the panel is thus ‘shaded’ by the aluminum top of the LSC: this shading becoming more pronounced and affecting a larger area as the sun rises (see Fig. 6). On the other hand, light incident on the bottom half of the panel is not shaded in this way. The ‘dip’ during the middle of the day is due to the sun occupying a position over the barrier such that the top bar of the aluminum frame of the barrier acts as a shading element, masking the panel from most of the direct light, and affects both top and bottom cells.

The North/South facing noise barriers do not show such a variation between the top and bottom cells. In this case, both top and the bottom PVs respond similarly throughout the day, and do not receive any direct solar illumination, but only are illuminated by the emissions of the LSC lightguide. Two 'dips' in the performance, one around 09:00 and one around 19:00 h are the result of the sun being partially blocked by the side support panels of the aluminum frame. At 09:00 on this specified date, the sun was positioned incident directly from the East. The additional sharp 'peaks' at 07:30 and 19:30 are a result of light directly scattered from the white vertical side edges of the lightguide: this will be discussed more in section 3.2.

3.2. Side: top vs bottom

The silicon PV cells that are compared here are TS and BS in Fig. 2 for both the East/West and North/East facing noise barriers. Here, the TS PV is located to the west side of the barrier and the BS PV is located to the east part of the barrier. The performance ratio comparison for those cases appears in Fig. 7.

Similar to the previous discussion of the more centrally mounted cells, in the North/South facing barriers the bottom and top PVs receive different intensities throughout the day. More specifically, during the first half of the day it is the top cells that receive relatively more light whereas in the second half of the day they receive less light. The two colored circles highlight this difference. The differences indicated in the green circle, which refers to the earlier part of the day, is caused by interference of the frame of the barrier. From the moment that the sun is rising (from the northeast part of the sky) until it reaches the eastern part of the sky (in position parallel to the barrier), the bottom cell which is positioned towards the east is shaded by the frame. This leads to higher amount of light for the top side cell which is facing west, therefore it is not similarly affected. This effect appears reversed in the later part of the day until the sun sets. This means greater amount of light for the bottom cell (see Fig. 7).

Inside the green circle of Fig. 7b appears a spike at about 7:30 in the morning. This spike is the result of the presence of a white scatterer placed on the short side of the LSC panels. This scatterer on the west edge of the LSC encounters direct sunlight incident on the LSC from the east. The sunlight not absorbed by the dye encounters the scatterer, which redirects some of this incident sunlight back to the panel. Because the scatter effects all wavelengths of incident light, including light beyond the limit of Red305 absorption (>600 nm), this means these longer wavelengths which are not absorbed by the dye that are trapped in the lightguide could travel for long distances, some even reaching the cell at the opposite end of the panel (note the small peak in the bottom cell in the early hours). This process is reversed later in the day, when the direct sun

from the west has its light scattered by the east mounted scatterer placed on the edge of the N/S facing LSC, with some of the scattered light traversing the entire length of panel to become incident on the top cell on the west side. These additional spikes are also noticeable in the more centrally mounted cells: see Fig. 5.

3.3. Top: middle vs side

In this section we compare the performance of the TM and TS silicon PV cells in Fig. 2 for both the East/West and North/East facing noise barriers. The performance ratio comparison for those cases appears in Fig. 8.

In the case of the East/West facing barrier, the more centrally mounted PV cell performs better than the more side mounted cell over the entire day. This difference is attributed to differences in the quality of the optical connection between the cell strips and the plate. This situation is similar in the North/South facing panels, but the optical connection seems to be more equal here.

3.4. Bottom: middle vs side

The silicon PVs that are compared here correspond to BM and BS in Fig. 2 for both the East/West and North/East facing noise barriers. The performance ratio comparison for these cases appears in Fig. 9.

The performance results of the bottom mounted cells are similar to those of the top mounted cells for both orientations. For the East/West facing barrier, the BM cell may receive more light because the frame obstructs part of the light reaching the side cell.

For the North/South facing barrier, the middle and side cells perform similarly during the greater part of the day. As described in section 3.2, the side cell is affected by the presence of the white scatterer at the panel edges: the frame blocks the light during the first part of the day while the scatter causes more light to reach the cell.

3.5. Extended period measurements

The East/West facing panels had two solar peaks during the day while the North/South panels only one. This resulted in different PV performance ratios depending on the cell position for the East/West facing panels, while the cells on the North/South panels showed similar performance ratios regardless of position. The direct, daily PR comparison between the TM and BM cells on the Red LSC panel for both orientations through the measurement period between 23/5/2015 and 8/12/2015 shows the different behavior for the cells: see Fig. 10. These results incorporate a variety of weather conditions, including periods of clouds and rain, but no snowfall.

These experiments have utilized large scale LSCs oriented in two extremum: exact E/W and N/S orientations. It would be very

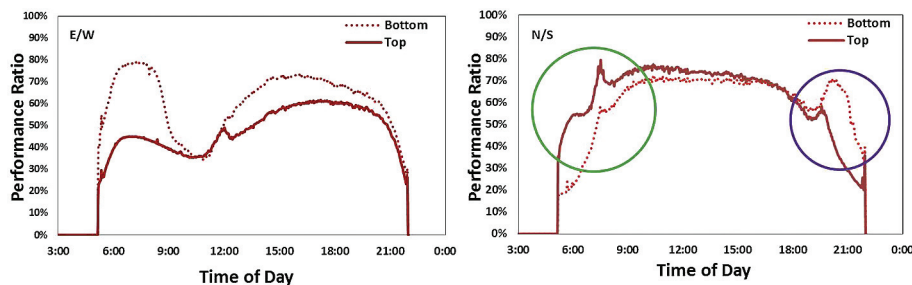


Fig. 7. Performance ratios of silicon PV cells mounted on the BS (dotted lines) and TS (solid lines) for barriers facing east/west (E/W) and north/south (N/S) as a function of the time of day on June 30, 2015.

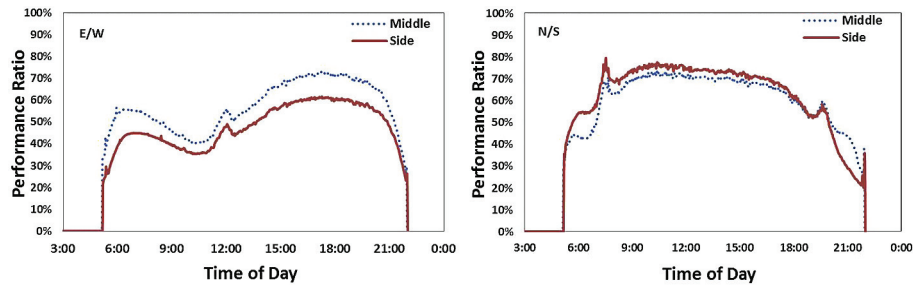


Fig. 8. Performance ratios of silicon PV cells mounted on the TM (dotted lines) and TS (solid lines) for barriers facing east/west (E/W) and north/south (N/S) as a function of the time of day on June 30, 2015.

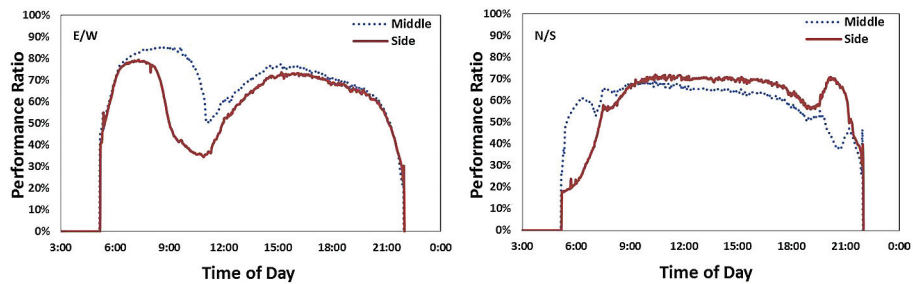


Fig. 9. Performance ratios of silicon PV cells mounted on the BM (dotted lines) and BS (solid lines) for barriers facing east/west (E/W) and north/south (N/S) as a function of the time of day on June 30, 2015.

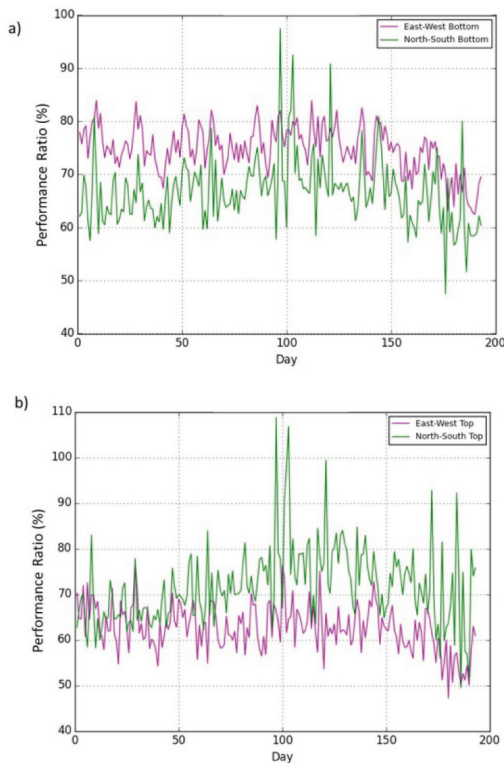


Fig. 10. Performance ratios for a) BM and b) TM mounted PV cells located on the East/West (pink) and North/South (green) facing panels for an almost 200 day period from May to December, 2015. (For interpretation of the references to colour in this figure legend, the reader is referred to the web version of this article.)

interesting in follow-up work to investigate the intermediate cases when the panels are not aligned along the compass axes, and performance at different latitudes. The tilt angle of 15° also impacts

performance, as this dictates when the frame will interfere with electricity generation. However, other constraints related to the blocking of sound, the primary function of the noise barrier, will go far in dictating how much this latter aspect can be altered.

A key feature of these noise barriers is their ability to accept light from either side for electrical generation. As can be seen from the data of the E/W facing panels, the performance in the morning and afternoon are approximately the same: it does not matter from where the sun shines, as long as light enters the surface of the lightguide, it may be processed. This work also clearly shows that regions not covered with photovoltaic cells should be painted with a white scattering layer to allow collection of otherwise non-absorbed light. The work presented in this paper will provide insight and guidance for the construction of future LSC demonstration objects to ascertain their commercial viability, both in the production of electrical power, but also in their aesthetic appeal, and improved ease of integration into the urban landscape.

4. Conclusions

We have presented the first data related to the Solar Noise Barrier (SONOB) project in Den Bosch, the Netherlands, which involves the monitoring of performance of two $5 \times 1 \text{ m}^2$ luminescent solar concentrator panels in two different colors oriented to face due North-South and East-West, each with a 15° tilt from the vertical. We have identified different performance responses in the silicon photovoltaic cells attached to the center and off-center locations on the top and bottom of the red lightguides. Due to the orientation, the North South panels suffer less from shading losses by the support frame compared to the East West oriented panels. This will have implications for the overall system design. The results of the data collected on the single day in June appear representative of the relative performances of the cells for the 200 day period recorded from May until early December. We demonstrate the importance of frame design to minimize self-shading in the first full-size LSC devices.

Acknowledgements

The authors would like to acknowledge the SONOB project funded partially by the TKI ZEGO program. They would also like to thank Stijn Verkuilen, Eppo Zuur, Walter Groenewald, and Peter Heijmans of Heijmans BV, Remco van der Heijden from Airbus DS, Alex Timmerman from Van Campen, and Menno van den Donker from SEAC for many helpful discussions.

References

- [1] B. Petter Jelle, C. Breivik, H. Drolsum Røkenes, Building integrated photovoltaic products: a state-of-the-art review and future research opportunities, *Sol. Energy Mater. Sol. Cells* 100 (2012) 69–96.
- [2] F. Frontini, P. Bonomo, A. Chatzipanagi, G. Verberne, M. van den Donker, K. Sinapis, W. Folkerts, BIPV product overview for solar façades and roofs, in: SUPSI SEAC, 2015, p. 47. The report may be downloaded at: http://www.seac.cc/fileadmin/seac/user/doc/SEAC-SUPSI_report_2015_-_BIPV_product_overview_for_solar_facades_and_roofs_1_.pdf (Accessed 26 September 2016).
- [3] W.H. Weber, J. Lambe, Luminescent greenhouse collector for solar radiation, *Appl. Opt.* 15 (1976) 2299–2300.
- [4] J.S. Batchelder, A.H. Zewail, T. Cole, Luminescent solar concentrators. 1: theory of operation and techniques for performance evaluation, *Appl. Opt.* 18 (1979) 3090–3110.
- [5] W.G.J.H.M. van Sark, K.W.J. Barnham, L.H. Slooff, A.J. Chatten, A. Büchtemann, A. Meyer, S.J. McCormack, R. Koole, D.J. Farrell, R. Bose, E.E. Bende, A.R. Burgers, T. Budel, J. Quilitz, M. Kennedy, T. Meyer, C.D.M. Donega, A. Meijerink, D. Vanmaekelbergh, Luminescent Solar Concentrators – a review of recent results, *Opt. Express* 16 (2008) 21773–21792.
- [6] M.G. Debije, P.P.C. Verbunt, Thirty years of luminescent solar concentrator research: solar energy for the built environment, *Adv. Energy Mater.* 2 (2012) 12–35.
- [7] F.M. Vossen, M.P.J. Aarts, M.G. Debije, Visual performance of red luminescent solar concentrating windows in an office environment, *Energy Build.* 113 (2016) 123–132.
- [8] M.G. Debije, V.A. Rajkumar, Direct versus indirect illumination of a prototype luminescent solar concentrator, *Sol. Energy* 122 (2015) 334–340.
- [9] L.H. Slooff, E.E. Bende, A.R. Burgers, T. Budel, M. Pravettoni, R.P. Kenny, E.D. Dunlop, A. Büchtemann, A luminescent solar concentrator with 7.1% power conversion efficiency, *Phys. Status Solidi - R.* 2 (2008) 257–259.
- [10] L. Desmet, A.J.M. Ras, D.K.G. De Boer, M.G. Debije, Monocrystalline silicon photovoltaic luminescent solar concentrator with 4.2% power conversion efficiency, *Opt. Lett.* 37 (2012) 3087–3089.
- [11] S.M. Reda, Stability and photodegradation of phthalocyanines and hematoporphyrin doped PMMA as solar concentrators, *Sol. Energy* 81 (2007) 755–760.
- [12] M.A. El-Shahawy, A.F. Mansour, Optical properties of some luminescent solar concentrators, *J. Mater. Sci. Mater. Elect.* 7 (1996) 171–174.
- [13] A.F. Mansour, Outdoor testing of luminescent solar concentrators in a liquid polymer and bulk plate of PMMA, *Polym. Test.* 17 (1998) 153–162.
- [14] S.M. El-Bashir, O.A. AlHarbi, M.S. AlSalhi, Thin-film LSCs based on PMMA nanohybrid coatings: device optimization and outdoor performance, *Int. J. Photoenergy* 2013 (2013) 10.
- [15] G. Seybold, G. Wagenblast, New perylene and violanthrone dyestuffs for fluorescent collectors, *Dyes Pigm.* 11 (1989) 303–317.
- [16] M.G. Debije, J.-P. Teunissen, M.J. Kastelijn, P.P.C. Verbunt, C.W.M. Bastiaansen, The effect of a scattering layer on the edge output of a luminescent solar concentrator, *Sol. Energy Mater. Sol. Cells* 93 (2009) 1345–1350.